THE JOURNAL OF PHYSICAL CHEMISTRY C

Article

pubs.acs.org/JPCC

Interpreting the Density of States Extracted from Organic Solar Cells Using Transient Photocurrent Measurements

Roderick C. I. MacKenzie,*[,†,‡] Chris G. Shuttle,[§] George F. Dibb,[∥] Neil Treat,[§] Elizabeth von Hauff,[⊥] Maxwell J. Robb,[#] Craig J. Hawker,[#] Michael L. Chabinyc,[§] and Jenny Nelson[∥,‡]

[†]Faculty of Engineering, University of Nottingham, Nottingham, Nottinghamshire NG7 2RD, U.K.

[‡]FRIAS, School of Soft Matter Research, University of Freiburg, Albertstraβe 19, 79104 Freiburg, Germany

[§]Materials Department, University of California Santa Barbara, Santa Barbara, California 93106-5050, United States

[∥]Department of Physics, Imperial College London, South Kensington Campus, London SW7 2AZ, U.K.

[⊥]Institute of Physics, Hermann-Herder-Str. 3a, D-79104 Freiburg, Germany

[#]Materials Research Laboratory, University of California, Santa Barbara, Santa Barbara, California 93106-5121, United States

Supporting Information

ABSTRACT: The energetic distribution of trapped carrier states (DoS) in organic photovoltaic (OPV) devices is a key device parameter which controls carrier mobility and the recombination rate; as such, it can ultimately limit device efficiency. Recent studies have attempted to measure the DoS from working OPV devices using transient photocurrent methods adapted from the time-of-flight (ToF) method originally developed to measure mobility in thick unipolar devices. While a method to extract the DoS from OPV devices using a simple optoelectronic means would be valuable, analysis is complicated by the presence of both electrons and holes in the bipolar organic solar cells. The presence of both carrier species leads to distortion of the extracted DoS due to (a) recombination losses removing carriers from the photocurrent transient thus changing its shape and (b) both LUMO and HOMO DoS features being observed simultaneously in any measurement. In this paper we use a detailed device model to determine the conditions under which the DoS can safely be extracted from the transient photocurrent from bipolar devices. We show that under conditions of reverse bias it is possible to extract the undistorted DoS from a working OPV device. We apply our method to estimate the DoS in a bulk heterojunction solar cell made of a novel low band gap, diketopyrrolopyrrole-based polymer blended with [6,6]-phenyl-C71-butyric acid methyl ester (PC71BM) and solar cells made of poly(3 hexylthiophene):phenyl-C61-butyric acid methyl ester (P3HT:PCBM) annealed over a range of temperatures.

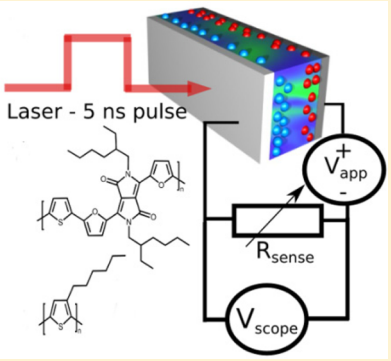

1. INTRODUCTION

Organic solar cells offer the potential of a low-cost,[1] mass-produced,[2−4], low-carbon source of electricity. Within the past five years largely through the development of narrow bandgap polymers[5] designed to maximize absorbed solar radiation, power conversion efficiencies have increased from 3%[6] to over 10.0%.[7] However, to further increase energy conversion efficiency, a larger proportion of the photogenerated charge carriers need to reach the contacts of the cell.[8] To achieve this, the carrier recombination lifetime (τ) and mobility (μ) of the materials must be maximized.[8] It is well-known that deep energetic traps,[9−13] in the distribution of electron and hole states will reduce the mobility.[9] Furthermore, it has recently been demonstrated that charge recombination[14−19] in organic photovoltaic (OPV) devices takes place via energetically deep carrier traps.[20−24] Thus, the ability to measure the energetic distribution of carrier trap states in a working OPV device is key to understanding both recombination and mobility in these material systems and thus to understanding why some materials produce devices with high collection efficiencies and some do not.[8] Previous studies have attempted to determine the DoS from working OPV devices using methods including capacitance−voltage techniques,[25] capacitance−frequency techniques,[26] sub-bandgap quantum efficiency measurements,[27] space-charge-limited current techniques,[28] and time-of-flight (ToF) methods.[17] However, none of these techniques have yet been able to reliably extract the DoS distribution from working cells. Capacitance−voltage measurements can only be performed on undoped or thick (unoptimized) devices;[29] capacitance−frequency measurements can only access very shallow traps;[30] sub-bandgap quantum efficiency measurements are hard to interpret because the matrix element may not be constant;[31] and space-charge limited techniques were developed to work on insulators while OPV materials are often unintentionally doped.[29] More recently, time-of-flight (ToF) photocurrent transient techniques,[32−34] originally applied to

Received: January 30, 2013
Revised: May 16, 2013

   dx.doi.org/10.1021/jp4010828 | J. Phys. Chem. C XXXX, XXX, XXX−XXX

probe the density of states in optically thick inorganic films, have been adapted to optically thin organic solar cells.[17] In the ToF technique[32] a thin sheet of charge pairs is photogenerated close to one contact by a laser pulse. Under a large applied field, carriers of one species are rapidly drawn to the closest contact, leaving carriers of the other species to propagate across the thick sample and generate a displacement photocurrent. As these carriers propagate across the device, some of the carriers become trapped and are subsequently released after a delay that depends on the trap energy. At long times around an order of magnitude later than the transit time, the current transient is dominated by the detrapping of these carriers from relatively shallow traps,[35,36] while current measured later is dominated by charge detrapping from deeper traps. Using an appropriate transform the current transient can thus be used to estimate the relative magnitude of the DoS as a function of energy.[32] A key condition to using the ToF technique in this way is that the device must be optically thick so that only one carrier species will be studied at a time. However, optically thick devices may differ in their internal microstructure and electronic processes compared to working solar cells and can additionally be difficult to fabricate. In an optically thin organic solar cell the laser pulse will excite electrons and holes throughout the entire device rather than only close to the contact.[23] As a result, the measured current transient at long times will contain current from both the detrapping of electrons and holes, preventing the clean measurement of either DoS distribution. Furthermore, the presence of the two carrier species will enable recombination during transit, and this can significantly distort the extracted DoS. Despite these difficulties, the measurement technique is the most simple and potentially most powerful method yet proposed to extract the DoS from a working device. Therefore, in this paper we investigate the conditions under which the transient current measurements can retain a faithful image of the DoS of either carrier type. To this end, we experimentally measure photocurrent transients from bulk heterojunction solar cells made from two different material systems over a range of measurement conditions. We then apply a macroscopic device model[23] to understand how the measurement conditions influence the apparent shape of the extracted DoS. We obtain a set of measurement conditions under which photocurrent transient techniques deliver a faithful estimate of the DoS in real devices. For clarity, we differentiate between ToF and transient photocurrent (TPC) by defining ToF as a technique used on optically thick cells with at least one blocking contact and TPC as a technique used on optically thin cells with nonblocking contacts.

2. EXPERIMENTAL SECTION

Transient photocurrent measurements were performed at 238 and 293 K on an optimized device made from the low bandgap material PDPP2FT blended with PC71BM at short circuit and at an applied bias of −2 V. We also studied a series of devices made from poly(3-hexylthiophene) (P3HT) blended with PCBM at a temperature of 293 K under short circuit, −1 V, and −2 V. Three P3HT:PCBM devices were studied in total, each with a different post processing annealing temperature applied (140 °C, 80 °C, and no annealing). The fabrication of these devices is described in detail in the Supporting Information. A diagram of the experimental TPC transient measurement system can be seen in Figure 1. It comprises of a solar cell, a voltage source (V_{app}), a 520 nm Nd:YAG laser, and a sense resistor (R_{sense}). The transients were obtained by biasing the

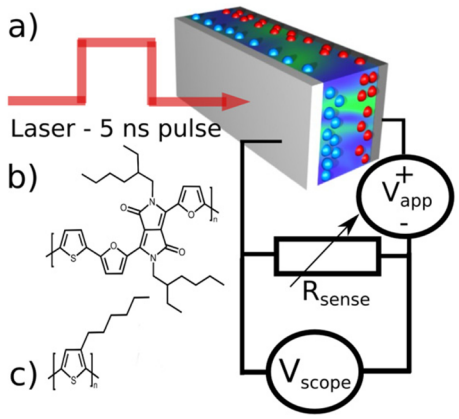

Figure 1. (a) A diagram of the TPC measurement system; the red and blue balls represent both electrons and holes being present in the cell at the same time. (b) The structure of the narrow bandgap polymer PDPP2FT. (c) The structure of P3HT.

system with the desired electrical bias then applying a short (5 ns) optical pulse from the laser. The resulting current transient is measured over R_{scense} using an oscilloscope.[23,37]

A diagram of a typical TPC transient, as would be measured by the experimental system, can be seen in Figure 2a. The

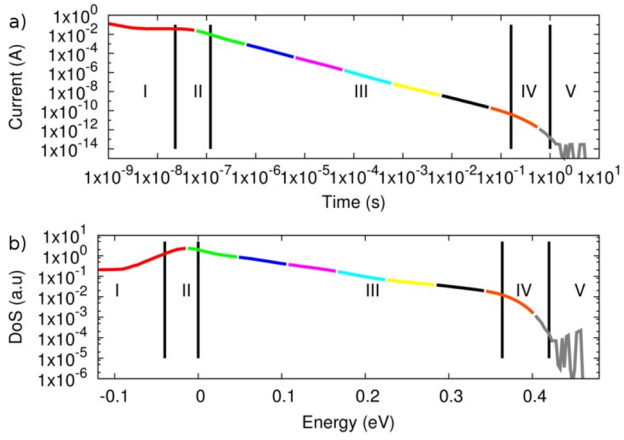

Figure 2. (a) An example of a typical TPC transient with the dark diode current removed. (b) The DoS extracted from the TPC transient in (a). The graph has been color coded so one can tell which parts of the DoS were formed from which time period in (a).

transient can be divided into five distinct regions. When the laser pulse illuminates the sample, free charge carriers are photogenerated throughout the solar cell, and they start to drift and diffuse to the contacts generating a current plateau (region I). As organic solar cells are quite thin (~100−250 nm), they generally have a high geometric capacitance, which means the RC response of the system often dominates this region. While the carriers travel to the contacts, trapping and detrapping of carriers occur. This retards the transport of some carriers, which causes the end of region I to drop in magnitude (region II). During regions I and II some carriers become trapped from transport states into energetically deep traps.

If these carriers do not recombine, they can detrap and produce a current (region III). As time increases, carriers detrap from progressively deeper traps. At very long times all carriers have either been extracted or recombined thus the transient ends (region IV). Finally, when all the photoexcited carriers

dx.doi.org/10.1021/jp4010828 | J. Phys. Chem. C XXXX, XXX, XXX−XXX

have left the device, the dark diode current remains. This has already been subtracted off Figure 2a; thus, the final region V consists only of noise. Regions I−II are commonly referred to as the pre-transit, and regions III−V are commonly referred to as the post-transit.

One of the most simple methods for estimating the DoS from experimental ToF data (as depicted in Figure 2a) is one first proposed by Seynhaeve,[33] later improved upon by Main[35] and applied to organic solar cells by Street.[17] The result of their work is that when the current is dominated by detrapping from a distribution of trap states, the DoS $g(E)$ is proportional to the product of the current $i(t)$ and time t

$$g(t) = \frac{i(t)t}{qvfkT} \tag{1}$$

where v is the volume of the sample, f is the fraction of states filled at each energy level, k is Boltzmann's constant, T is the temperature, and q is the charge on an electron. In the derivation of this equation it is assumed that at time t only the carriers at energy E fully detrap;[35] there is no carrier retrapping and no recombination. The relation

$$E(t) = kT \ln(v_0 t) \tag{2}$$

is used to relate the time (t) at which a carrier is extracted to the trap depth in terms of energy E, where v_0 is the attempt to escape frequency. During the derivation[33] it is also assumed that the relative number of carriers which are captured into each trap level depends upon the density of states at that energy level and not the trap's energetic depth; i.e., this assumes the rate of carrier transport downhill in energy does not depend upon the energetic gradient. Thus, the relative carrier population captured at each energy level is proportional to the DoS distribution.[35,36] To obtain an absolute DoS distribution the proportion of traps filled (f) must be known just after the laser pulse has ended. This is difficult to accurately estimate; therefore, eq 1 is usually normalized to a maximum of one, and a relative DoS distribution is obtained. Then the energy of 0 meV is defined as the mobility edge and positive energies represent trapped states below the mobility edge. The transient depicted in Figure 2a has been transformed with eqs 1 and 2, and the result is shown in Figure 2b. The data in Figures 2a,b have been color-coded to show which time periods correspond to which energy levels. As the transformation assumes that the current is dominated by detrapping, this approach is only valid in region III where the current should be dominated by detrapping of trapped carriers. Regions I and II are dominated by transport, region IV is dominated by recombination, and region V is dominated by noise; thus, the transform is not valid in these regions.

3. RESULTS

Figure 3 shows the DoS extracted from the PDPP2FT:PC71BM cell at short circuit (0 V) and −2 V by using eq 1. The value of the carrier attempt to escape rate (v_0) required to calibrate the energy axis was (eq 2) was obtained by adjusting v_0 until the DoS functions at both temperatures lay on top of each other; this yielded a value of $v_0 = 1 \times 10^7$ s^{-1}. The region between −0.1 and 0.05 eV is an artifact from the pre-transit and the RC response of the system—it obscures any DoS structure between 0.0 and 0.05 eV. In reverse bias at 0.2 eV the extracted DoS starts to trend upward. Recently, Street presented TPC data collected on the PCDTBT:PCBM material

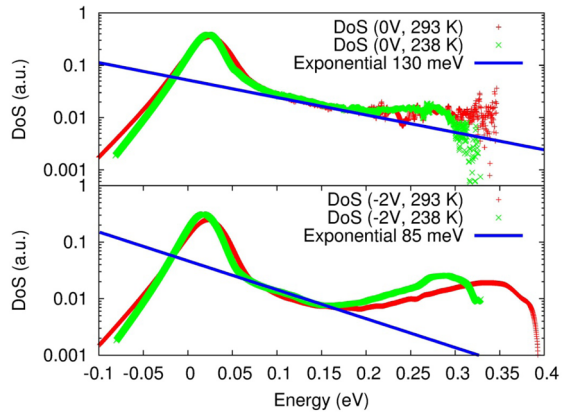

Figure 3. A plot of the DoS extracted directly from a PDPP2FT:PC71BM solar cell at −2 V and at short circuit (0V).

system,[17] where he also observed such behavior. This could potentially be attributed to a deep trap in the material system[23,38] but will be discussed in detail later. It can be seen that a shallow tail of slope 85 meV is extracted at −2 V and a broader tail of 130 meV is extracted at short circuit. Previously, it has been suggested that in a device with asymmetric mobilities the carriers of the species with the higher mobility will be swept out of the device first, leaving behind the carrier species with the lower mobility to form the post-transit current from which the DoS can be extracted.[17] Our observation of two distinct tail slopes cannot be accounted for if this explanation is true under all circumstances.

Figure 4 plots the measured DoS functions for a series of P3HT:PCBM cells which were unannealed (red), annealed at

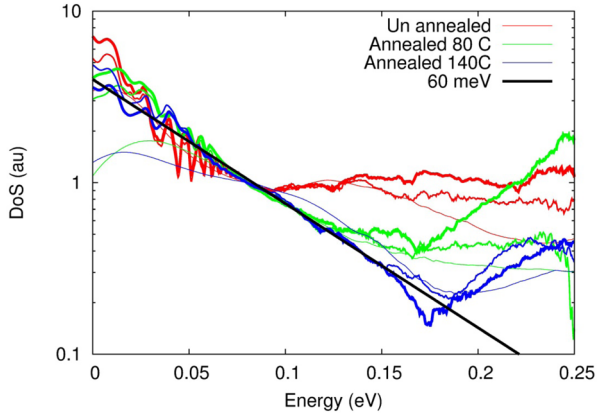

Figure 4. A plot of the DoS extracted from TPC measurements obtained from series of P3HT:PCBM solar cells which were unannealed (red), annealed at 80 °C (green) and annealed at 140 °C (blue). The TPC measurements were performed at short circuit (thin lines), −1 V (thick lines), and −2 V (thickest lines).

80 °C (green) and annealed at 140 °C (blue) after fabrication. The TPC measurements were performed at short circuit (thin lines), −1V (thick lines) and −2V (thickest lines).

It can be seen that between 0 and 0.08 eV the slope of the DoS when measured in reverse bias for all annealing temperatures is 60 meV. This is in line with previous experimental data for the P3HT:PCBM material system which reported values of 57 meV[24] and 60 meV.[23] The two exceptions to this trend are the annealed devices when measured at short circuit. Thus, as with the

dx.doi.org/10.1021/jp4010828 | J. Phys. Chem. C XXXX, XXX, XXX−XXX

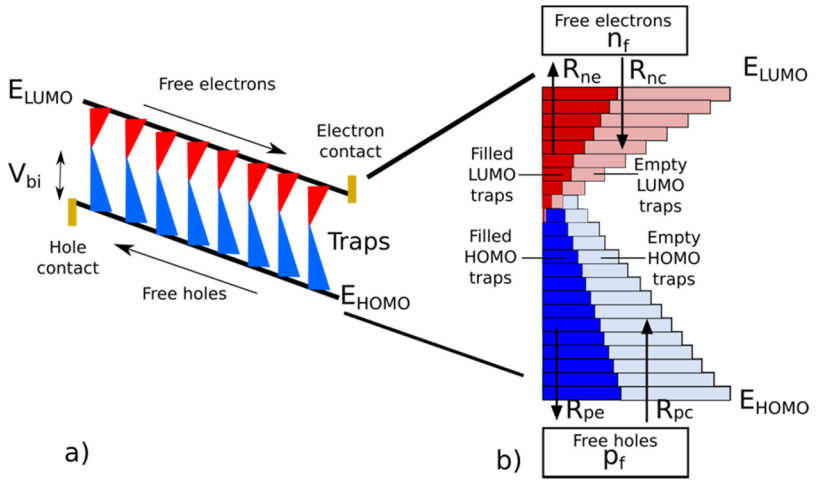

Figure 5. (a) A 1D band diagram of the device model showing the distributions of trap states below the LUMO and above the HOMO. (b) A 0D energy space slice through the 1D model, showing the discretized trap distribution. R_{nc}, R_{ne}, R_{pc}, and R_{pe} represent electron capture, electron escape, hole capture, and hole escape rates, respectively. Note the filled trap states in (b) approximate the distribution of the DoS because the carrier trapping rate is not dependent upon trap depth (this is discussed in the text above). The Shockley–Read–Hall recombination pathways have not been drawn for brevity.

PDPP2FT:PC71BM device we observe a voltage dependence of the extracted DoS. Between 0.08 and 0.17 eV the extracted DoS of the unannealed device flattens out, while the extracted DoS for the devices annealed at 80 and 140 °C continues to fall. This observed decrease in deep states upon annealing could potentially be the reason why the hole mobility and efficiency of P3HT:PCBM devices increase when annealed[39] (this will be investigated later in the paper). Between 0.13 and 0.25 eV the DoS extracted from all the devices is a strong function of voltage. Again, this is not consistent with the concept that only the DoS of the slowest charge type is being accessed.[17] The above experimental data pose a number of questions: (1) Why does applied bias appear to change the slope of the extracted DoS? (2) Does neglecting the presence of the two carrier species during the above analysis limit the usefulness of the experimental data? (3) Is the LUMO or HOMO DoS being accessed? (4) What influence do asymmetric electron and hole mobilities have on the transient. (5) What does the apparent reduction in deep states in the P3HT:PCBM upon annealing mean? In the remainder of the paper we address these questions using a numerical diode model and determine what information our experimental measurements have provided about the DoS in these devices. This results in a simple experimental way to access and understand the DoS in functioning organic solar cells.

4. THEORETICAL ANALYSIS

In the following pages, we use a macroscopic device model that incorporates the effects of charge trapping in tail states[23] to simulate TPC transients. For the simulations we set the HOMO and LUMO DoS tail slopes to be 100 and 50 meV, respectively, and attempt to extract the HOMO and LUMO distributions from the simulated transients under various measurement conditions. We use these simulations to establish the conditions in which the TPC measurements in section 3 provide reliable information about the DoS distribution in these organic solar cells. Initially, we investigate a simulated device with symmetric electron and hole parameters (excluding DoS tail slopes); then we vary the device parameters to investigate the effects of material properties on our ability to extract the DoS from the transients. The numerical model has previously been described in detail elsewhere.[23] Briefly, it solves Poisson's equation and the bipolar drift diffusion[23,40,41] equations in 1D to account for transport and electrostatic effects.[23] Carrier recombination and trapping in the active layer are described using the Shockley–Read–Hall mechanism.[23] The distribution of LUMO and HOMO states are described as two exponential distributions[22−24,41,42] of form

$$g_{\mathrm{LUMO}}(E) = N_{\mathrm{LUMO}} \exp\left(\frac{-E}{U_{\mathrm{LUMO}}}\right) \quad (3)$$

$$g_{\mathrm{HOMO}}(E) = N_{\mathrm{HOMO}} \exp\left(\frac{-E}{U_{\mathrm{HOMO}}}\right) \quad (4)$$

where E is the distance between the mobility edge and the trap level, LUMO/HOMO is the slope of the DoS distribution, and LUMO/HOMO is the density of states at the mobility edge. A 1D band diagram of the model is shown in Figure 5a, and a diagram of the exponential trap distribution is shown in Figure 5b. Further detail about the model including a full list of device parameters can be found in the Supporting Information. The simulated device has a short circuit current of J_{sc} = 9.5 mA cm^{-2}, an open circuit voltage of V_{oc} = 0.60 V, and a fill factor of FF = 0.62; the device had a power conversion efficiency of 3.0% at 1 sun illumination.

4.1. Why Does Applied Bias Appear To Change the Slope of the extracted DoS? Previously, it has been suggested that in a TPC measurement the charge carrier with the lowest mobility will dominate the long time scale part of the transient, and therefore TPC can be used to measure the trap distribution of the slowest charge carrier at short circuit. However, in Figures 3 and 4, it can be seen that the extracted DoS is dependent upon the applied voltage, and therefore the above statement cannot be correct. To understand this voltage dependence, TPC simulations were performed over a range of applied biases between −2.0 and +2.0 V in the dark. The resulting extracted DoS function can be seen in Figure 6. With an applied bias of −2 V the 100 meV HOMO tail can be

dx.doi.org/10.1021/jp4010828 | J. Phys. Chem. C XXXX, XXX, XXX−XXX

extracted, and as the voltage increases, the extracted tail slope decreases.

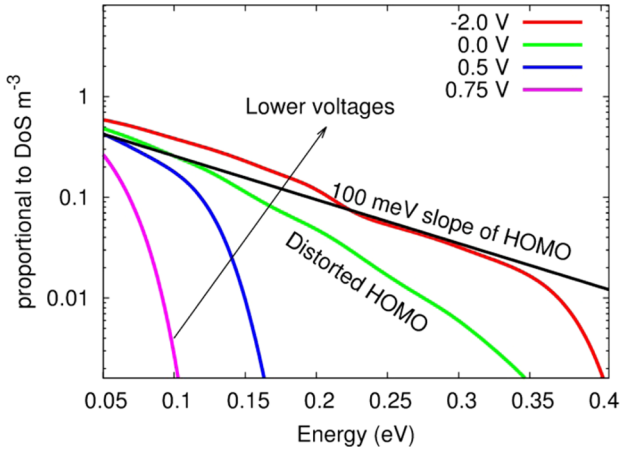

Figure 6. Influence of simulated applied bias on the extracted DoS in the dark. The HOMO DoS can only be extracted at negative voltages because recombination is low allowing carriers to detrap and reach the contacts without recombining.

The reason the extracted DoS is a function of voltage can be understood by examining Figure 7 which plots the extracted

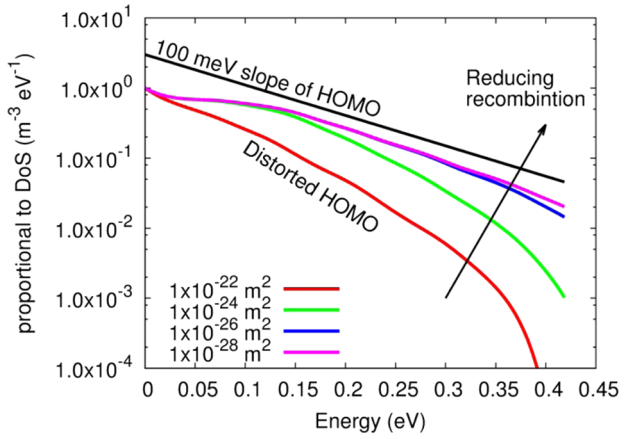

Figure 7. Extracted DoS as short circuit as a function of recombination cross section. It can be seen that the DoS is distorted at short circuit when recombination is high (large cross section).

DoS at short circuit as a function of recombination cross section. The electron and hole recombination cross sections determine the rate at which the free electrons (holes) can recombine with the trapped holes (electrons). A smaller cross section means less recombination. As recombination is reduced within the device the HOMO distribution can be more accurately recovered. This indicates that at short circuit recombination is distorting the extracted DoS. At large negative biases the extracted HOMO DoS is not affected by recombination for three reasons: (1) the applied negative bias reduces the background carrier population in the device thus reducing recombination; (2) the higher field removes detrapped and free carriers from the device more quickly giving them less time to recombine; and (3) the applied field sweeps away any free carriers remaining from the photo-excitation which have not become trapped, again reducing recombination.

In summary, at short circuit recombination can distort the DoS extracted from a TPC transient. By performing TPC measurements at high electric fields in reverse bias, recombination is minimized and distortion to the DoS reduced.

4.2. Is the LUMO or HOMO DoS Being Accessed in Experimental Measurements? We can understand why only the HOMO and not the LUMO will be measured at −2 V in Figure 6 and gain a better understanding of TPC transients by examining Figure 8. This figure plots snapshots of the carrier

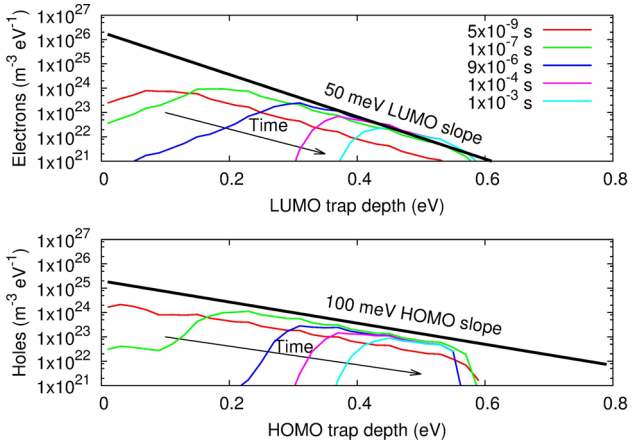

Figure 8. Evolution with time of the distributions of carriers within the LUMO and HOMO as a function of energy. It can be seen that the HOMO initially captures more carriers; this is because the tail is broader and has more states at each energy level. This energy slice is taken from the middle of the device.

population within the HOMO and LUMO traps in energy space taken from the center of the device between 5×10^{-9} and 1×10^{-3} s. At 5×10^{-9} s the laser has just turned off, and the distribution of carriers in the LUMO and HOMO is approximately exponential. It can be seen that the broader HOMO tail captures more charge carriers at each energy level. This is because the carrier trapping rate in Shockley−Read−Hall (SRH) theory is proportional to the number of trap states at any given energy. Because the HOMO captured more carriers at each energy level during the pre-transit, it will therefore be able to supply more charge to the post-transit transient per unit time. This will mean holes will dominate the TPC transient and thus only the HOMO DoS would be observed in any experimental measurement. According[20] to eq 2, carriers in shallower traps will take less time to detrap than carriers in deep traps. This can be seen at 1×10^{-7} s between 0.0 and 0.15 eV where there is a reduced carrier density close to the mobility edge. Even though at 1×10^{-7} s the laser pulse has finished, it can be seen that the magnitude of the carrier density at energies below 0.15 eV is still increasing. This is because carriers are escaping the shallow energy traps, becoming free and then being recaptured into deeper energy traps. Once a carrier is captured into a deep trap, it takes longer for it to escape; hence, there is a redistribution of carriers from shallow traps to deep traps. Even though the device is biased at −2 V to minimize recombination, it can be seen that there is still a reduction of carriers in very deep traps as time progresses due to annihilation (0.57−0.60 eV in the hole distribution). Previously, it has been implied[17] that all carrier traps need to be filled to extract the DoS correctly, as can be seen from the figure the initial distribution of carriers automatically follows

dx.doi.org/10.1021/jp4010828 | J. Phys. Chem. C XXXX, XXX, XXX−XXX

the DoS distribution so filling all the traps is not necessary; indeed, only about 2% of the DoS states are initially occupied. The simulated device considered so far had the same absolute magnitude of carrier traps at the mobility edge $N_{LUMO} = N_{HOMO} = 5 \times 10^{25}$ m^{-3} eV^{-1}. Figure 9 considers the case when the

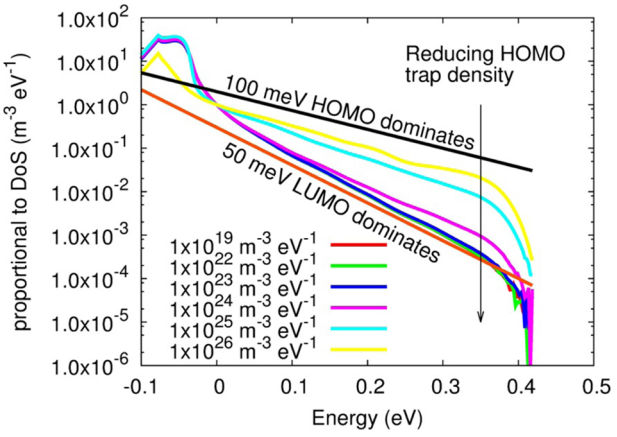

Figure 9. DoS extracted when the magnitude of the HOMO tail is reduced. The HOMO dominates at high trap densities; however, as the density of the HOMO traps falls, the LUMO tail becomes observable. The tail with the most states per unit energy will dominate the extracted DoS because it can capture more carriers during the pre-transit phase and thus contribute more current to the post-transit current. These simulations were performed at an applied bias of −2 V.

absolute magnitude of the HOMO DoS is reduced from 1×10^{26} to 1×10^{19} m^{-3} eV^{-1}, while keeping the magnitude of the electron DoS fixed at 5×10^{25} m^{-3} eV^{-1}. As the magnitude of the hole DoS is reduced, it is apparent that the tail slope of the extracted DoS shifts from 100 to 50 meV. As described above, this is because the DoS with more states per energy level will capture more carriers in the pre-transient and be able to dominate the post-transient current. This opens up an interesting possibility of making OPV bulk heterojunction devices with a low concentration of one component of the blend in order to selectively measure the DoS of the other component. This would however only be possible for BHJ materials which produce a measurable photocurrent when either the acceptor or donor formed a significantly larger component of the blend. An analogous evaluation of the time evolution of charges in dye-sensitized solar cells has been performed by Barzykin and Tachiya.[43]

4.3. What Influence Do Asymmetric Mobilities Have on the Extracted DoS? If a carrier spends a long time in the device, there is a high probability that it will recombine or retrap thus distort the TPC transient. To investigate the influence carrier transport has on the DoS extracted from TPC transients, TPC simulations were performed in reverse bias (−2 V) with the absolute value of the effective free electron mobility varied from 1×10^{-9} to 1×10^{-5} m^2 V^{-1} s^{-1}, while the effective free hole mobility was maintained at a value of 1×10^{-5} m^2 V^{-1} s^{-1}. It was found that when the electrons had a very low mobility, neither the HOMO or LUMO could be recovered from the TPC transient because the electrons remain within the device, distorting the hole current through recombination. When the applied voltage was increased from −2 to −10 V reducing the time carriers spend in the device, the HOMO tail could again be recovered. If one examines the experimental data from the PCDTBT:PCBM device in Figure 3 at short circuit, it can be seen that there is a plateau between 0.2 and 0.35 eV; this resembles the plateau between 0.2 and 0.4 eV in the simulated data in Figure 10. This suggests that the DoS obtained from the

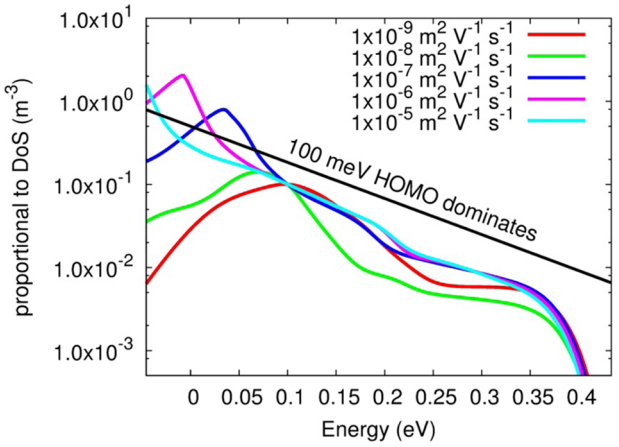

Figure 10. Extracted DoS when the simulated LUMO mobility is reduced by 6 orders of magnitude, at −2 V applied bias in the dark.

PCDTBT:PCBM device at short circuit is distorted by recombination due to the carriers not being extracted from the device quickly enough. At −2 V a Gaussian shape starts to appear between 0.2 and 0.4 eV in the PCDTBT:PCBM DoS. Similar features have been observed by other authors.[38] We attribute this feature to dynamic carrier effects caused by fast recombination. Dynamic voltage dependent features in the DoS are provided in the Supporting Information.

5. UNDERSTANDING THE P3HT:PCBM DATA

In section 4 we showed that when the extracted DoS no longer appears to change as a function of negative bias, the extracted DoS is a reliable estimation of the trap state distribution; with this in mind we can now interpret the P3HT:PCBM data in Figure 4. The P3HT:PCBM cells annealed at 80 and 140 C (blue and green lines in Figure 4) show a significant change in the extracted DoS between 0.0 and 0.15 eV when the applied bias is changed from short circuit to −1 V . However, when the applied bias is changed from −1 to −2 V, the extracted DoS between 0.0 and 0.15 eV does not change. This suggests that recombination at short circuit is high enough to distort the extracted DoS in the P3HT:PCBM cell, but an accurate DoS is being extracted at more negative voltages in this region. Between 0.125−0.25 eV (0.17−0.25 eV) the DoS extracted from the devices annealed at 140 °C (80 °C) varies as a function of applied voltage for all biases; thus, from this data we cannot be sure the true DoS is being accessed in this energy range. If the experimentally extracted DoS for the unannealed P3HT:PCBM solar cell (red lines, Figure 4) is examined between 0.13 and 0.25 eV, it can be seen that the extracted DoS appears to change significantly as a function of voltage; thus, again this is probably not a true representation of the DoS in this energy region. However, between 0 and 0.13 eV the extracted DoS remains unchanged as the applied bias is varied. This suggests that the observed exponential tail between 0 and 0.1 eV and the small plateau between 0.1 and 0.13 eV are real features of the DoS. Upon annealing, the plateau between 0.1 and 0.13 eV disappears. It has previously been reported that as a P3HT:PCBM solar cell is annealed the hole mobility increases and the efficiency increases;[39,44,45] this reduction in

dx.doi.org/10.1021/jp4010828 | J. Phys. Chem. C XXXX, XXX, XXX−XXX

deep trap states at 0.1−0.13 eV could be the reason for this increase in mobility.

6. CONCLUSION

In this work, we measured TPC transients produced from an optimized PDPP2FT:PC71BM solar cell and a series of P3HT:PCBM solar cells annealed at different temperatures. We then extracted the apparent DoS from the measured transients. The extraction of the DoS was complicated due to the presence of two carrier species. In order to aid understanding of the experimental results, we used a microscopic device model to perform a series of TPC simulations. In general, we found that the DoS which can capture most carriers during the pre-transit will produce most current during the post-transit. Hence, in general the DoS with most states will be observed. It was found that the extracted DoS of the PDPP2FT:PC71BM cell varied as a function of applied voltage. Our simulations suggested that this was due to recombination and transport effects distorting the transient. The DoS extracted from the P3HT:PCBM cell changed significantly between short circuit and −1 V; however, it remained constant when the applied voltage was increased from −1 to −2 V . Therefore, at negative voltages larger than −1 V the true DoS was extracted. The DoS in all three P3HT:PCBM cells (unannealed, annealed at 80 °C, and annealed at 140 °C) flattened out at deeper energies; however, these regions became voltage dependent, which suggests the true DoS was not being measured. We observed a small voltage independent plateau in the unannealed cell which disappeared upon annealing. This could be the cause for the increased hole mobility and efficiency observed in P3HT:PCBM solar cells. In general, we find that TPC data can be used to extract the DoS from OPV devices. However, the measurements should be performed over a range of negative voltages, and only when the extracted DoS stops changing as a function of voltage, can one be sure the true DoS distribution is being observed and not carrier dynamic-based effects. Finally, we recommend that TPC measurements be combined with either detailed device modeling or complemented with other experimental techniques[38] to confirm both the slope of the exponential tails and presence of deep traps.

■ ASSOCIATED CONTENT

Supporting Information

Fabrication information and device parameters for the simulated device. This material is available free of charge via the Internet at http://pubs.acs.org.

■ AUTHOR INFORMATION

Corresponding Author

*E-mail roderick.mackenzie@nottingham.ac.uk; Tel (+44) 01157484434.

Notes

The authors declare no competing financial interest.

■ ACKNOWLEDGMENTS

R.M. gratefully acknowledges the support of the U.K. Engineering and Physical Sciences Research Council EPSRC Grant No. EP/F056710/1. G.D. acknowledges the support of an EPSRC case award. We thank Imperial College High Performance Computing Service for providing computational support. J.N. thanks the Royal Society for the award of an Industrial Fellowship. M.C. and C.S. acknowledge support as part of the Center for Energy Efficient Materials, an Energy Frontier Research Center funded by the U.S. Department of Energy, Office of Science, Office of Basic Energy Sciences, under Award DE-SC0001009. Solar cell fabrication was performed using the MRL Central Facilities, which are supported by the MRSEC Program of the NSF under Award DMR05-20415, a member of the NSF funded Materials Research Facilities Network. C.J.H. and M.R. thank the NSF SOLAR program for partial support of this work (CHE-1035292). N.D.T. acknowledges support from the ConvEne IGERT Program (NSF-DGE 0801627) and a NSF Graduate Research Fellowship. We also acknowledge the support of the TSB via the SCALLOPS project.

■ REFERENCES

(1) Emmott, C. J.; Urbina, A.; Nelson, J. Effects of Annealing and Degradation on Regioregular Polythiophene-Based Bulk Heterojunction Organic Photovoltaic Devices. *Sol. Energy Mater. Sol. Cells* **2012**, *97*, 14−21.

(2) Krebs, F. C.; Gevorgyan, S. A.; Gholamkhass, B.; Holdcroft, S.; Schlenker, C.; Thompson, M. E.; Thompson, B. C.; Olson, D.; Ginley, D. S.; Shaheen, S. E.; et al. A Round Robin Study of Flexible Large-Area Roll-to-Roll Processed Polymer Solar Cell Modules. *Sol. Energy Mater. Sol. Cells* **2009**, *93*, 1968−1977.

(3) Girotto, C.; Moia, D.; Rand, B.; Heremans, P. Photovoltaic Devices: High-Performance Organic Solar Cells with Spray Coated Hole-Transport and Active Layers. *Adv. Funct. Mater.* **2011**, *21*, 2−2.

(4) Girotto, C.; Rand, B.; Genoe, J.; Heremans, P. Exploring Spray Coating as a Deposition Technique for the Fabrication of Solution-Processed Solar Cells. Sol. *Energy Mater. Sol. Cells* **2009**, *93*, 454−458.

(5) Woo, C. H.; Beaujuge, P. M.; Holcombe, T. W.; Lee, O. P.; Frechet, J. M. J. Incorporation of Furan into Low Band-Gap Polymers for Efficient Solar Cells. *J. Am. Chem. Soc.* **2010**, *132*, 15547−15549.

(6) Green, M. A.; Emery, K.; Hishikawa, Y.; Warta, W. Solar Cell Efficiency Tables (version 30). *Prog. Photovoltaics* **2007**, *15*, 425−430.

(7) Green, M. A.; Emery, K.; Hishikawa, Y.; Warta, W.; Dunlop, E. D. Solar Cell Efficiency Tables (version 39). *Prog. Photovoltaics* **2012**, *20*, 12−20.

(8) Azimi, H.; Senes, A.; Scharber, M. C.; Hingerl, K.; Brabec, C. J. Charge Transport and Recombination in Low-Bandgap Bulk Heterojunction Solar Cell Using Bis-Adduct Fullerene. *Adv. Energy Mater.* **2011**, *16*, 1162−1168.

(9) Bässler, H. Charge Transport in Disordered Organic Photoconductors. *Phys. Status Solidi B* **1993**, *175*, 15−55.

(10) Bohnenbuck, B.; von Hauff, E.; Parisi, J.; Deibel, C.; Dyakonov, V. Current-Limiting Mechanisms in Polymer Diodes. *J. Appl. Phys.* **2006**, *99*, 024506.

(11) Roichman, Y.; Tessler, N. Generalized Einstein Relation for Disordered Semiconductors - Implications for Device Performance. *Appl. Phys. Lett.* **2002**, *80*, 1948−1950.

(12) Stelzl, F. F.; Würfel, U. Modeling the Influence of Doping on the Performance of Bulk Heterojunction Organic Solar Cells: One-Dimensional Effective Semiconductor Versus Two-dimensional Donor/Acceptor Model. *Phys. Rev. B* **2012**, *86*, 075315.

(13) Tessler, N.; Roichman, Y. Amorphous Organic Molecule/Polymer Diodes and Transistors—Comparison Between Predictions Based on Gaussian or Exponential Density of States. *Org. Electron.* **2005**, *56*, 200−210.

(14) Hilczer, M.; Tachiya, M. Unified Theory of Geminate and Bulk Electron−Hole Recombination in Organic Solar Cells. *J. Phys. Chem. C* **2010**, *114*, 6808−6813.

(15) Groves, C.; Greenham, N. C. Bimolecular Recombination in Polymer Electronic Devices. *Phys. Rev. B* **2008**, *78*, 155205.

(16) Koster, L. J. A.; Mihailetchi, V. D.; Blom, P. W. M. *Appl. Phys. Lett.* **2006**, *88*, 052104.

(17) Street, R. A. Localized State Distribution and its Effect on Recombination in Organic Solar Cells. *Phys. Rev. B* **2011**, *84*, 075208.

(18) Wagenpfahl, A.; Deibel, C.; Dyakonov, V. Organic Solar Cell Efficiencies Under the Aspect of Reduced Surface Recombination Velocities. *IEEE J. Sel. Top. Quantum Electron.* **2010**, *16*, 1759−1763.
(19) Cowan, S. R.; Street, R. A.; Cho, S.; Heeger, A. J. Transient Photoconductivity in Polymer Bulk Heterojunction Solar Cells: Competition between Sweep-out and Recombination. *Phys. Rev. B* **2011**, *83*, 035205.
(20) Shockley, W.; Read, W. T. Statistics of the Recombinations of Holes and Electrons. *Phys. Rev.* **1952**, *87*, 835−842.
(21) Kuik, M.; Nicolai, H. T.; Lenes, M.; Wetzelaer, G.-J. A. H.; Lu, M.; Blom, P. W. M. Determination of the Trap-Assisted Recombination Strength in Polymer Light Emitting Diodes. *Appl. Phys. Lett.* **2011**, *98*, 093301.
(22) Kirchartz, T.; Pieters, B. E.; Kirkpatrick, J.; Rau, U.; Nelson, J. Recombination via Tail States in Polythiophene:Fullerene Solar Cells. *Phys. Rev. B* **2011**, *83*, 115209.
(23) MacKenzie, R. C. I.; Shuttle, C. G.; Chabinyc, M. L.; Nelson, J. Extracting Microscopic Device Parameters from Transient Photocurrent Measurements of P3HT:PCBM Solar Cells. *Adv. Energy Mater.* **2012**, *2*, 662−669.
(24) Foertig, A.; Rauh, J.; Dyakonov, V.; Deibel, C. Shockley Equation Parameters of P3HT:PCBM Solar Cells Determined by Transient Techniques. *Phys. Rev. B* **2012**, *86*, 115302.
(25) Garcia-Belmonte, G.; Boix, P. P.; Bisquert, J.; Sessolo, M.; Bolink, H. J. Simultaneous Determination of Carrier Lifetime and Electron Density-of-States in P3HT:PCBM Organic Solar Cells under Illumination by Impedance Spectroscopy. *Sol. Energy Mater. Sol. Cells* **2010**, *94*, 366−375.
(26) Ecker, B.; Nolasco, J. C.; Pallars, J.; Marsal, L. F.; Posdorfer, J.; Parisi, J.; von Hauff, E. Degradation Effects Related to the Hole Transport Layer in Organic Solar Cells. *Adv. Funct. Mater.* **2011**, *21*, 2705−2711.
(27) Street, R. A.; Song, K. W.; Northrup, J. E.; Cowan, S. Photoconductivity Measurements of the Electronic Structure of Organic Solar Cells. *Phys. Rev. B* **2011**, *83*, 165207.
(28) Nikitenko, V. R.; Heil, H.; von Seggern, H. Space-Charge Limited Current in Regioregular Poly-3-Hexyl-Thiophene. *J. Appl. Phys.* **2003**, *94*, 2480−2485.
(29) Kirchartz, T.; Gong, W.; Hawks, S. A.; Agostinelli, T.; MacKenzie, R. C. I.; Yang, Y.; Nelson, J. Sensitivity of the Mott−Schottky Analysis in Organic Solar Cells. *J. Phys. Chem. C* **2012**, *116*, 7672−7680.
(30) Khelifi, S.; Decock, K.; Lauwaert, J.; Vrielinck, H.; Spoltore, D.; Piersimoni, F.; Manca, J.; Belghachi, A.; Burgelman, M. Investigation of Defects by Admittance Spectroscopy Measurements in Poly (3 hexylthiophene):(6,6)-phenyl C[sub 61]-Butyric Acid Methyl Ester Organic Solar Cells Degraded Under Air Exposure. *J. Appl. Phys.* **2011**, *110*, 094509.
(31) Gong, W.; Faist, M. A.; Ekins-Daukes, N. J.; Xu, Z.; Bradley, D. D. C.; Nelson, J.; Kirchartz, T. Influence of Energetic Disorder on Electroluminescence Emission in Polymer: Fullerene Solar Cells. *Phys. Rev. B* **2012**, *86*, 024201.
(32) Reynolds, S.; Smirnov, V.; Finger, F.; Main, C.; Carius, R.; Optoelectron., J. Transport and Instabilities in Microcrystalline Silicon Films. *Adv. Mater.* **2005**, *7*, 91−98.
(33) Seynhaeve, G. F.; Barclay, R. P.; Adriaenssens, G. J.; Marshall, J. M. Post-Transit Time-of-Flight Currents as a Probe of the Density of States in Hydrogenated Amorphous Silicon. *Phys. Rev. B* **1989**, *39*, 10196−10205.
(34) Main, C.; Reynolds, S.; Badran, R. I.; Marshall, J. M. High Resolution Density of States Spectroscopy in Semiconductors by Exact Post-Transit Current Analysis. *J. Appl. Phys.* **2000**, *88*, 1190−1192.
(35) Main, C.; Nesheva, D. Transient Photocurrent Techniques as a Means of Characterising Amorphous Semiconductors. *J. Optoelectron. Adv. Mater.* **2001**, *3*, 655−664.
(36) Scher, H.; Montroll, E. W. Anomalous Transit-time Dispersion in Amorphous Solids. *Phys. Rev. B* **1975**, *12*, 2455−2477.
(37) Shuttle, C. G.; Treat, N. D.; Douglas, J. D.; Fréchet, J.M. J.; Chabinyc, M. L. Deep Energetic Trap States in Organic Photovoltaic Devices. *Adv. Energy Mater.* **2012**, *2*, 111−119.
(38) Carati, C.; Bonoldi, L.; Po, R. Density of Trap States in Organic Photovoltaic Materials from LESR Studies of Carrier Recombination Kinetics. *Phys. Rev. B* **2011**, *84*, 245205.
(39) Li, G.; Shrotriya, V.; Yao, Y.; Yang, Y. Investigation of Annealing Effects and Film Thickness Dependence of Polymer Solar Cells Based on Poly(3-hexylthiophene). *J. Appl. Phys.* **2005**, *98*, 043704.
(40) MacKenzie, R.; Lim, J. J.; Bull, S.; Sujecki, S.; Kent, A. J.; Larkins, E. C. The Impact of Hot-Phonons on the Performance of 1.3μm Dilute Nitride Edge-Emitting Quantum Well Lasers. *J. Phys.: Conf. Ser.* **2007**, *92*, 012068.
(41) MacKenzie, R. C. I.; Kirchartz, T.; Dibb, G. F. A.; Nelson, J. Modeling Nongeminate Recombination in P3HT:PCBM Solar Cells. *J. Phys. Chem. C* **2011**, *115*, 9806−9813.
(42) Nelson, J. Diffusion-limited Recombination in Polymer-Fullerene Blends and its Influence on Photocurrent Collection. *Phys. Rev. B* **2003**, *67*, 155209.
(43) Barzykin, A. V.; Tachiya, M. Mechanism of Charge Recombination in Dye-Sensitized Nanocrystalline Semiconductors: Random Flight Model. *J. Phys. Chem. B* **2002**, *106*, 4356.
(44) Vanlaeke, P.; Swinnen, A.; Haeldermans, I.; Vanhoyland, G.; Aernouts, T.; Cheyns, D.; Deibel, C.; D'Haen, J.; Heremans, P.; Poortmans, J.; et al. P3HT/PCBM Bulk Heterojunction Solar Cells: Relation Between Morphology and Electro-Optical Characteristics. *Sol. Energy Mater. Sol. Cells* **2006**, *90*, 2150−2158.
(45) Ebadian, S.; Gholamkhass, B.; Shambayati, S.; Holdcroft, S.; Servati, P. Effects of Annealing and Degradation on Regioregular Polythiophene-Based Bulk Heterojunction Organic Photovoltaic Devices. *Sol. Energy Mater. Sol. Cells* **2010**, *94* (12), 2258−2264.